Proceedings of the Thirtieth AAAI Conference on Artificial Intelligence (AAAI-16)

Bayesian Inference of Recursive Sequences of Group Activities from Tracks

Ernesto Brau,[1] Colin Dawson,[2] Alfredo Carrillo,[3] David Sidi,[3] Clayton T. Morrison[3]
[1]Computer Science Department, Boston College; brauavil@bc.edu
[2]Department of Mathematics, Oberlin College; cdawson@oberlin.edu
[3]School of Information, University of Arizona; {isaac85,dsidi,claytonm}@email.arizona.edu

Abstract

We present a probabilistic generative model for inferring a description of coordinated, recursively structured group activities at multiple levels of temporal granularity based on observations of individuals' trajectories. The model accommodates: (1) hierarchically structured groups, (2) activities that are temporally and compositionally recursive, (3) component roles assigning different subactivity dynamics to subgroups of participants, and (4) a nonparametric Gaussian Process model of trajectories. We present an MCMC sampling framework for performing joint inference over recursive activity descriptions and assignment of trajectories to groups, integrating out continuous parameters. We demonstrate the model's expressive power in several simulated and complex real-world scenarios from the VIRAT and UCLA Aerial Event video data sets.

1 Introduction

Human activity recognition comprises a range of open challenges and is a very active research area (Aggarwal and Ryoo 2011; Vishwakarma and Agrawal 2013; Sukthankar et al. 2014), spanning topics from visual recognition of individual behavior (Poppe 2010), pairwise interactions among individuals participating in different roles in a joint activity (Barbu et al. 2012; Kwak, Han, and Han 2013), coordinated sequences of actions as expressions of planned activity (Geib and Goldman 2009), and multiple groups of individuals interacting across broad time scales. In this paper, we address the last of these, presenting a framework for automatically constructing an interpretation of high-level human activity structure as observed in surveillance video, across multiple, interleaved instances of activities. We assume that lower-level visual processing provides high quality tracks of individuals moving through the scene. Our goal is to construct accurate descriptions of the events in the video at different levels of granularity, based on the tracks alone. We develop a probabilistic generative model that combines multiple features that to our knowledge have not been previously incorporated into a single framework for joint inference. To wit: (1) Activities have *composite structure* with *roles* representing semantically distinct aspects of the overall activity structure. (2) Activities are described *hierarchically* and *recursively*, entailing *multiple levels of granularity* both in time and membership. (3) Arbitrarily sized groups of actors participate in activities and fulfill roles. (4) Hierarchical descriptions and temporally changing groupings consist of the *best joint explanation* of the full set of individual trajectories, as found via posterior probabilistic inference.

The rest of the paper is organized as follows. In the next section, we review prior research, with a focus on work modeling group membership, hierarchically structured activities, and the identification of roles. In Section 3 we present our probabilistic generative model. In Section 4 we present an MCMC sampling framework for performing joint inference using the model. In Section 5 we evaluate the model on synthetic and real-world data from the VIRAT (Oh et al. 2011) and UCLA Aerial Event (Shu et al. 2015) video data sets, demonstrating the model's expressive power and effectiveness. We conclude with a discussion of future work.

2 Related Work

A number of researchers have proposed models that distinguish the different roles that individuals play in a coordinated activity (Ryoo and Aggarwal 2011; Barbu et al. 2012; Lan, Sigal, and Mori 2012; Kwak, Han, and Han 2013). These models capture the semantics of activities with component structure. It can be difficult to scale role identification in scenes with an arbitrary number of individuals, in particular while properly handling identification of non-participants (Kwak, Han, and Han 2013). A consequence of our joint inference over role assignments and groups is that our model naturally distinguishes and separates participants of different activities playing different roles.

Considerable work has been devoted to developing more expressive models in which activities are decomposed into hierarchical levels of description, across different spatial and temporal granularities. Some prior models account for a specific number of hierarchical levels of description, with up to 3 levels being a popular choice (Choi and Savarese 2012; Lan et al. 2010; Chang, Krahnstoever, and Ge 2011; Cheng et al. 2014). Other models permit a potentially greater number of levels of activity description, but the activity hierarchy is fixed prior to inference (Kwak, Han, and Han 2013; Garate et al. 2014; Zaidenberg, Boulay, and Bremond 2012). In only a few cases, including our model, are the levels of ac-

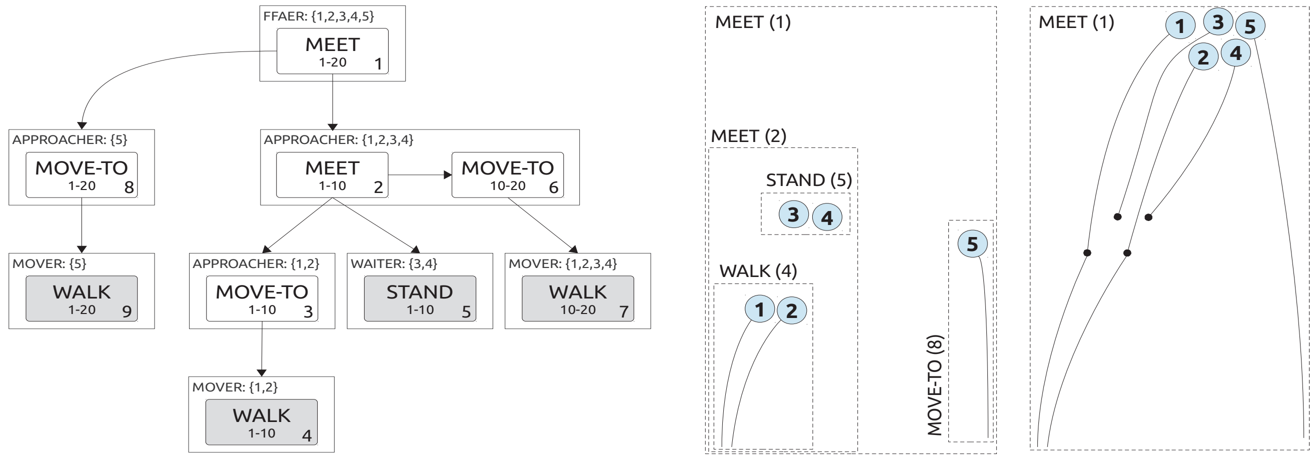

(a) Example activity tree (b) $t = 5$ (c) $t = 20$

Figure 1: This example depicts five synthetic trajectories and the corresponding activity tree representation. Each node in the activity tree (a) represents an activity. The central label indicates the activity name, with the time interval for the activity underneath. Each node is also numbered with a unique ID, which is displayed in the bottom-right corner of each node rectangle. Shaded nodes indicate physical activities. The outer rectangles represent *activity sequences*, whose roles and set of participants are displayed in the top left corner of their rectangles. For example, node 2 is activity C_2 with label $a_2 = \text{MEET}$, start time $s_2 = 1$, and end time $e_2 = 10$. Node 2 is part of an activity sequence realizing the role of APPROACHER by individuals $\mathcal{Z}_2 = \{1, 2, 3, 4\}$. In (b) and (c) we show two frames of the corresponding scene. Each circle represents an individual (1–5), and the curves are their paths on the ground plane. The dotted rectangles represent activities performed by the individuals inside them, labeled with their activity name and activity tree node number. For example, we can see in (b), at time $t = 5$, individuals 1 and 2 are walking together (node 4) to meet (node 2) with individuals 3 and 4, who are standing (node 5). All this happens while all individuals are participating in another global meeting together (node 1). By frame $t = 20$, depicted in (c), all participants are meeting. (Note: to simplify the presentation here, we omit the root FFA activity from the example activity tree in (a).)

tivity description assessed during inference (Lin et al. 2010; Ryoo and Aggarwal 2011).

A third branch of work has been devoted to modeling activities not just among individuals, but involving groups of actors. In some models, activities include groups, but interactions are still considered between individuals within groups (Choi and Savarese 2012; Lan et al. 2010; Zhang et al. 2013; Odashima et al. 2012; Zhu et al. 2011). Other models allow for activities to be performed between groups themselves (Chang, Krahnstoever, and Ge 2011; Chang et al. 2010). Still others, including our model, take group activity modeling a step further, allowing for arbitrary numbers of participants in groups, provided they satisfy group membership criteria while performing the activity (Lin et al. 2010; Kwak, Han, and Han 2013; Shu et al. 2015; Zhang et al. 2012).

Two recent papers, one by Ryoo and Aggarwal (2011) and one by Shu et al. (2015), come closest to accommodating the combination of features in our model. Both have developed methods for simultaneous inference of group structure with roles in hierarchically structured activities. One key difference between the two is that the former, like our model, can flexibly accommodate multiple levels of activity description in the course of inference, while the latter is restricted to two fixed levels of description during inference (one for group activities, and the other for their member roles). A crucial difference with our approach is that we consider the possibility of detecting multiple occurrences of the same type of activity description in a scene, and these descriptions are integrated into a single probabilistic joint model in order to influence inference of the overall activity structure. While activities described in Ryoo and Aggarwal (2011) have hierarchical component structure with roles, their model does not accommodate more than one top level activity (i.e. assault, meet, robbery, etc.) occurring during the course of the video, nor changes in group membership by individuals over such high-level activities.

3 Model

We present a probabilistic generative model describing how coordinated activities by groups of individuals give rise to the observed physical trajectories of the actors involved. In Section 3.1 we introduce some terminology. Then, in Section 3.2 we give precise definitions of the representations employed by our model for activities, groups, activity sequences, and spatial trajectories. Next, in Section 3.3, we define the factors in the joint probability distribution that comprise the generative model. Finally, in Section 3.4 we define the specific activities that are used to model the scenes that we use for evaluation in Section 5.

3.1 Terminology

Activities are optionally composed of other activities. For example, the canonical MEET activity in our model consists of multiple participating groups, each of which must MOVE-TO the location of the meeting, unless they are already there, and then possibly wait (STAND) until one or more other groups arrive. Engaging in a MOVE-TO activity requires the group to carry out a sequence of WALK and RUN activities. The semantics of a WALK or RUN is, in turn, characterized by the group's physical trajectory in space.

A scene is described as an *activity tree*, which has a recursive structure, much as a syntactic tree describes the recursive phrase structure of a natural language sentence, but with an added temporal component. An example of such a tree is depicted in Figure 1(a). We refer to the more abstract, "nonterminal" activities that are defined in terms of other activities as *intentional*, and the "leaf" activities that are defined in terms of observable movement as *physical*.

Participants in an intentional activity are divided into *subgroups*, each of which plays a particular *role* with respect to the parent activity. Carrying out a particular role entails engaging in a sequence of subactivities, each of which may be physical or intentional. In intentional activities, the group may be decomposed further into smaller subgroups, each with their own role in the subactivity, and so on. The *sequence* of subactivities performed by participants in a role is constrained (either deterministically or stochastically) according to the dynamics associated with the role. In cases where a role in a parent activity may be realized as a sequence that includes the same activity type as the parent, the structure is recursive, and allows for arbitrary nesting of activities at different time scales. For example, in Figure 1, a group of individuals participating in a MEET activity performs a sub-MEET of their own.

Physical activities are associated with *group trajectories*, which are coupled either via shared membership or when an intentional activity requires their coordination. An individual, j, has an observed trajectory that is generated as a sequence of connected sub-trajectories, one for each physical activity in which j participates, and which is constrained to be near the respective group trajectory. An example of an observed set of individual trajectories is shown in Figure 1(c).

An important feature of our model is that group trajectories are not explicitly represented during inference. The assertion that there is some group trajectory induces correlations among the individual trajectories of the members, but we average over all possible group trajectories (marginalizing them out) when computing the posterior probability of a description. This allows activity descriptions with different numbers of groups to be compared based on the posterior probabilities of their activity trees alone, without needing to deal with probability densities with different numbers of dimensions.

3.2 Representation

Activities Formally, an activity is a tuple $C = (a, s, e)$, where a is an activity label (e.g., WALK), and $s, e \in \mathbb{R}^+$ are the start and end time of the activity, respectively. The simplest activities are *physical* activities, e.g., walking, running and standing, which directly constrain the motion of a group of individuals over an interval of time. For example, a RUN activity is expected to yield trajectories with speeds corresponding to typical human running. We denote the set of physical activity labels by $\mathcal{A}_{\text{phys}}$. Similarly, *intentional* activities include MEET and MOVE-TO. We denote the set of intentional activity labels by $\mathcal{A}_{\text{int}}$. The complete set of activities is denoted by $\mathcal{A} = \mathcal{A}_{\text{phys}} \cup \mathcal{A}_{\text{int}}$.

Groups The set of participants in activity C is denoted by $\mathcal{Z}_C \subset \mathbb{N}$. We let $J_C = |\mathcal{Z}_C|$, the size of the group. This set is partitioned into subgroups, $\{\mathcal{Z}_1, \ldots, \mathcal{Z}_{K_C}\}$, where the number K_C of subgroups is bounded only by the number of individuals, J_C, in the group. When specifying the probability model, it is convenient to work instead with the indicator variables, $\mathbf{z}_C = (z_{C1}, \ldots, z_{CJ_C})$, where z_{Cj} indicates which of the K_C subgroups participant j is affiliated with. Note that $\mathbf{z}_C$ contains exactly the same information as the partition. In the following description, we omit the subscript C for readability.

Activity Sequences Each subgroup within activity C performs a *sequence* of subactivities. For example, a subgroup in a MEET might perform a sequence of two subactivities: first, MOVE-TO a designated meeting location, and then STAND in that location while meeting with other subgroups, who may have also approached that location. Alternatively, one of the subgroups could be involved in a side meeting, with further subgroups that approach and merge with each other before their union merges with another subgroup of the top-level MEET. Figure 1 provides such an example.

The sequences of subactivities performed by subgroups are governed by *roles*. Each subgroup k is assigned a role from a set $\mathcal{R}_a$ defined by the parent activity a. Roles govern the dynamics of the sequence of subactivities that each group carries out, via a set of parameters associated with that role. The parameters for role r specify what the allowable activities are in the activity sequence of a group carrying out that role, as well as hard or soft constraints involving what order the activities occur in. The subgroup of the example MEET activity above would be assigned the role of APPROACHER, which prescribes a MOVE-TO followed by a STAND. In this case the constraint on the order of subactivities is deterministic, with the only degrees of freedom being the times at which transitions take place. These constraints can be represented by a Markov chain with a degenerate initial distribution and a transition matrix with only one nonzero off-diagonal entry per column. More general initial and transition distributions will give rise to softer constraints on activity sequences.

Trajectories Ultimately, each physical activity, realized over the interval $[s, e]$, is associated with a *group trajectory*, denoted by $\mathbf{x}$, which is a 2 by $e - s + 1$ array specifying a 2-dimensional position on the ground plane for each time index between s and e inclusive. The group trajectory represents the central tendency of the members' individual trajectory segments during the interval $[s, e]$. Since individual j's path depends on the sequence of activities it participates in, each individual trajectory $\mathbf{y}_j$ consists of segments, $\mathbf{y}_j^{(0)}, \ldots, \mathbf{y}_j^{(I_j)}$, consecutive pairs of which must be connected at *transition points*, $y_{*j}^{(1)}, \ldots, y_{*j}^{(I_j)}$, where $y_{*j}^{(i)}$ denotes the start of segment i and the end of segment $i-1$.

3.3 Generative Model

We now describe the generative process for activities. The high-level process has three steps: (1) recursive expansion of intentional activities, (2) generation of group trajectories for the set of physical activities, and (3) generation of individual trajectories conditioned on the group assignments and group trajectories.

Overview In the first step of activity generation, each intentional activity gives rise to one or more child activity sequences: one for each subgroup of participants involved in the parent activity. Each child sequence is assigned a role, based on the parent activity type. Subgroups and role assignments occur jointly. The choice of role governs the sequence of activities that the subgroup engages in, by specifying a Markov transition function. Each segment of an activity sequence may be a physical activity or another intentional activity. Each intentional activity in the sequence is recursively expanded until only physical activities are generated.

As a working example for this stage of the process, we consider the MEET activity at node 1, at the root of the tree in Figure 1(a). Node 1 has two child sequences corresponding to the two subgroups involved in the meeting, both carrying out the APPROACHER role. One of those child sequences consists of just a single MOVE-TO activity, while the other consists of two activities: a MEET, followed by a MOVE-TO. In general, a special top-level root activity, a "free-for-all" (FFA), comprises all actors and has a duration over the entire video. All other activities are children of the root FFA. (To simplify the example tree in Figure 1(a), we removed the parent FFA.) The details of this tree expansion are given in "Generating the Activity Tree", below.

We make a conditional independence assumption by supposing that the contents of a parent activity fully specify the distribution of possible child sequences, and that child sequences are conditionally independent of each other given their parent. Since child sequences can contain other intentional activities, activity generation is a recursive process, which bottoms out when no intentional activities are generated.

In the second step of the generative process, group trajectories are generated for each physical activity. This process must satisfy two constraints: (a) physical activity trajectories that share members and that border in time must be spatially connected; and (b) groups that need to physically interact as co-participants in an intentional activity, such as a MEET, must have trajectories that intersect at the appropriate points in time. Due to these constraints it is not feasible to generate group trajectories conditionally independently given the activity tree. Instead they are generated jointly according to a global Gaussian Process with a covariance kernel that depends on the activity tree in such a way as to enforce the key constraints. The details of this process are given in "Generating Group Trajectories", below.

For the example tree in Figure 1(a), four group trajectory segments are needed, one for each physical activity leaf node. Since WALK activity 9 is part of a meeting in which its participants must meet with the participants in WALK activity 7, the group trajectories for 7 and 9 must end in the same location. Similarly, WALK 4 must end where STAND 5 is located.

In the final step of the generative process, the individual trajectories are realized, conditioned on the set of group trajectories. Here, conditional independence is possible, with each individual's trajectory depending only on the sequence of group trajectories for physical activities in which that individual is a participant. This process is detailed in Section "Generating Individual Trajectories".

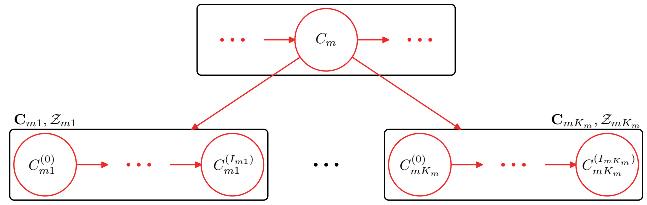

Figure 2: Graphical model for an intentional activity. The set $\mathcal{Z}_m$ of participants of activity C_m is partitioned into groups $\mathcal{Z}_{m1}, \ldots \mathcal{Z}_{mK_m}$ via the indicator vector $\mathbf{z}_m$. Each group is assigned a role, r_{mk}, and performs an activity sequence $\mathbf{C}_{mk} = (C_{mk}^{(0)}, \ldots, C_{mk}^{(I_{mk})})$, $k = 1, \ldots, K_m$.

Generating the Activity Tree Let $C_m = (a_m, s_m, e_m)$ be a parent intentional activity, where m indexes the set of activities. Its participant set $\mathcal{Z}_m$ (by relabeling, we assume that $\mathcal{Z}_m = \{1, \ldots, J_m\}$) is divided into subgroups, where the jth participant of C_m is assigned to group z_{mj}, and the distinct realized groups are numbered 1 through K_m. We let $\mathbf{z}_m = (z_{m1}, \ldots, z_{mJ_m})$, which defines a partition of $\mathcal{Z}_m$ into K_m subgroups, $\{\mathcal{Z}_{m1}, \ldots, \mathcal{Z}_{mK_m}\}$, with $\mathcal{Z}_{mk} = \{j \in \mathcal{Z}_m \mid z_{mj} = k\}$. Subgroup k is assigned role $r_{mk} \in \mathcal{R}$, and we define $\mathbf{r}_m = (r_{m1}, \ldots, r_{mK_m})$.

The kth subgroup, which has participants $\mathcal{Z}_{mk}$ and role r_{mk}, produces an activity sequence according to the stochastic process associated with r_{mk}, which has parameters $\boldsymbol{\pi}_{r_{mk}}$, a Markov transition function, and $\mathbf{T}_{r_{mk}}$, an initial activity distribution. Denote the resulting sequence by $\mathbf{C}_{mk} = (C_{mk}^{(0)}, \ldots, C_{mk}^{(I_{mk})})$, where I_{mk} is the number of jumps generated by the process, and the $C_{mk}^{(i)}$ are activity tuples, $C_{mk}^{(i)} = (a_{mk}^{(i)}, s_{mk}^{(i)}, e_{mk}^{(i)})$, where $s_{mk}^{(i)} = e_{mk}^{(i-1)}$. Figure 2 illustrates the graphical model of this production.

To summarize, the grouping, role assignment, and child activity sequences within activity C_m are generated according to $p(\mathbf{z}_m, \mathbf{r}_m, \mathbf{C}_m \mid C_m, \mathcal{Z}_m)$, which factors as

$$p(\mathbf{z}_m \mid a_m, \mathcal{Z}_m) p(\mathbf{r}_m \mid a_m) \prod_{k=1}^{K_m} p(\mathbf{C}_{mk} \mid s_m, e_m), \quad (1)$$

where we define $\mathbf{C}_m = (\mathbf{C}_{m1}, \ldots, \mathbf{C}_{mK_m})$. We assume that roles are assigned independently, so that $p(\mathbf{r}_m \mid a_m) = \prod_{k=1}^{K_m} p(r_{mk} \mid a_m)$. Additionally, we model the partition of $\mathcal{Z}_m$ into subgroups using a Chinese Restaurant Process (CRP), whose concentration parameter α_{a_m} depends on the activity label. That is, we let $p(\mathbf{z}_m \mid a_m, \mathcal{Z}_m)$ be the CRP mass function with parameter α_{a_m}. Each segment $C_{mk}^{(i)}$ of $\mathbf{C}_{mk}$ that is an intentional activity is expanded and its members are subdivided recursively according to (1), replacing C_m with $C_{mk}^{(i)}$ and $\mathcal{Z}_m$ with $\mathcal{Z}_{mk}$. Once all expansions contain exclusively physical activities, the recursion has bottomed out. The resulting tree consists of all intentional activities $C_1, \ldots, C_M$, all physical activities, $C_{M+1}, \ldots, C_{M+N}$, and, for each intentional activity $m = 1, \ldots, M$, its membership partition $\mathbf{z}_m$, role assignments $\mathbf{r}_m$, and subgroup activity sequences $\mathbf{C}_m$. We denote this complete tree by Λ, whose prior distribution is

$$p(\Lambda) = \prod_{m=1}^{M} p(\mathbf{z}_m, \mathbf{r}_m, \mathbf{C}_m \mid C_m, \mathcal{Z}_m). \tag{2}$$

Generating Group Trajectories The leaves of the activity tree are all physical activities, each of which is associated with a group trajectory. In general, the endpoints of different group trajectories are *not* independent (given Λ), since they may be constrained to start or end at the same location. Consequently, we define a joint distribution on all of the group trajectory endpoints, and, conditioned on their endpoints, we treat their interiors as independent.

We model the interiors as realizations of Gaussian processes (Rasmussen and Williams 2006) with the squared-exponential kernel function. This results in trajectories that are generally smooth, but flexible enough to allow for different kinds of motion. We use different scale parameters σ_{a_m} depending on the activity a_m, which determines the rate of change of the trajectory.

We specify dependencies among the set of trajectory endpoints by first defining an undirected weighted graph $\mathcal{G}$ over the endpoints. We use this graph to construct a constraint matrix over transition points by interpreting the sum of the weights on the shortest path between two nodes as distances. We then apply a positive semidefinite isotropic covariance kernel point-wise to the distance matrix to transform the distances into covariances.

Let $\mathbf{x}_m \in \mathbb{R}^{2(e_m - s_m + 1)}$ represent the sequence of ground-plane positions that make up the group trajectory for activity m. Abusing notation slightly, we will write $x_{*m}^{(s)}$ and $x_{*m}^{(e)}$ for both the endpoints of a group trajectory and the corresponding node in $\mathcal{G}$. We introduce three kinds of edges on $\mathcal{G}$: temporal, transitional, and compositional. Two nodes are connected by a *temporal* edge when they belong to the same physical activity. The start of an activity, $x_{*m}^{(s)}$, is connected to the end of another activity, $x_{*m'}^{(e)}$, by a *transitional* edge when they correspond to the same moment in time and the corresponding activities share at least one participant. Finally, two endpoints are connected by a *compositional* edge if they correspond to the same moment in time and have a common ancestor that specifies they must coincide, e.g., in a MEET activity, all participants must *end* in the same location. All transitional and compositional edges have weight (or "distance") zero, corresponding to the constraint that the connected edges must correspond to the same trajectory position. The weight assigned to temporal edges is a function of the time elapsed during the intervening physical activity and the σ associated with the activity label (e.g., "slower-moving" activities having lower weights, corresponding to a stronger dependence between the positions of their endpoints). Figure 3 shows an example $\mathcal{G}$.

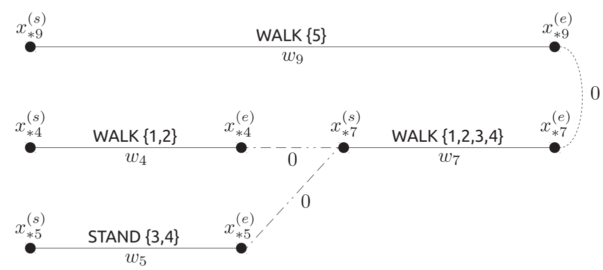

Figure 3: Constraint graph for the example activity tree in Figure 1. The nodes in the graph represent endpoints for group trajectories, labeled according to the numbering in the tree; e.g., $x_{*9}^{(s)}$ is the starting endpoint for node 9. Solid lines represent temporal edges, dashed lines are transitional edges, and dotted lines are compositional edges (see Section 3.3, "Generating Group Trajectories"). For clarity, temporal edges are labeled with their corresponding physical activity name. According to this graph, the distance between $x_{*5}^{(s)}$ and $x_{*9}^{(s)}$ is $w_5 + w_7 + w_9$, meaning that activities 5 and 9 must start in locations separated by a STAND and two WALKs.

Having defined $\mathcal{G}$ we can compute a distance matrix $\mathbf{D}$ for the set of physical activity endpoints, where the entry $d_{ii'}$ is the sum of the weights along the shortest path in $\mathcal{G}$ from node i to node i'. If no path exists between two nodes, the distance is set to ∞. We then transform $\mathbf{D}$ into a covariance matrix $\mathbf{\Phi}$ by applying the covariance function $\phi_{ii'} = \kappa(d_{ii'}) = \lambda e^{-d_{ii'}^2}$. The locations of the set of group trajectory endpoints $\mathbf{X}_* = (x_{*M+1}^{(s)}, x_{*M+1}^{(e)}, \ldots, x_{*M+N}^{(s)}, x_{*M+N}^{(e)})$ is distributed as $\mathbf{X}_* \mid \Lambda \sim \mathcal{N}(\mathbf{0}, \mathbf{\Phi})$. Conditioned on the endpoints, the interiors are mutually independent, so that

$$p(\mathbf{X}_{-*} \mid \mathbf{X}_*) = \prod_{m=M+1}^{M+N} p(\mathbf{x}_{-*m} \mid x_{*m}^{(s)}, x_{*m}^{(e)}), \tag{3}$$

where $\mathbf{x}_{-*m}$ is the vector of interior points of trajectory $\mathbf{x}_m$ and $\mathbf{X}_{-*} = (\mathbf{x}_{-*M+1}, \ldots, \mathbf{x}_{-*M+N})$. Each $\mathbf{x}_{-*m}$ is generated according to the Gaussian process for activity m; i.e., $\mathbf{x}_{-*m} \mid x_{*m}^{(s)}, x_{*m}^{(e)}$ is normally distributed. Finally, the distribution over the physical trajectories $\mathbf{X} = (\mathbf{x}_{M+1}, \ldots, \mathbf{x}_{M+N})$ factorizes as

$$p(\mathbf{X} \mid \Lambda) = p(\mathbf{X}_{-*} \mid \mathbf{X}_*) p(\mathbf{X}_* \mid \Lambda). \tag{4}$$

Using the fact that factors in (4) are normally distributed, we can easily see that $\mathbf{X}$ also has a normal distribution.

Generating Individual Trajectories As described above, individual j participates in physical activity sequence $\mathbf{C}_{(j)}$, which has the sequence of group trajectories $\mathbf{X}_j = (\mathbf{x}_j^{(1)}, \ldots, \mathbf{x}_j^{(I_j)})$. The individual trajectory $\mathbf{y}_j$ consists of

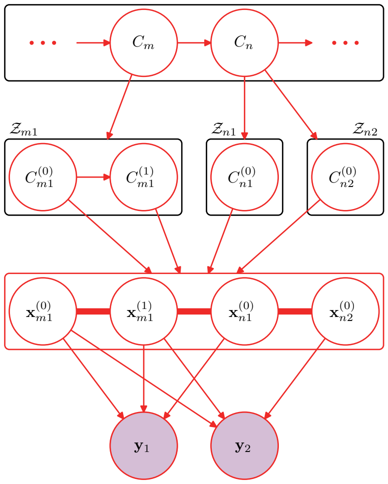

Figure 4: Graphical model for the generation of trajectories. This example shows a sequence of activities with two activities C_m and C_n. C_m has a single child with individuals Z_{m1} performing a sequence of two physical activities $C^{(0)}_{m1}$ and $C^{(1)}_{m1}$, while C_n is divided into two groups, each of which performs a single activity, culminating in physical activities $C^{(0)}_{n1}$ and $C^{(0)}_{n2}$. Each corresponding group trajectory $\mathbf{x}^{(0)}_{m1}, \mathbf{x}^{(1)}_{m1}, \mathbf{x}^{(0)}_{n1}$, and $\mathbf{x}^{(0)}_{n2}$ potentially depends on *all* physical activities, as well as being fully connected with each other (represented in the graph by thick red edges). Finally, individual trajectories $\mathbf{y}_1$ and $\mathbf{y}_2$ only depend on group trajectories whose physical activities contained their individuals.

segments, $\mathbf{y}^{(1)}_j, \ldots, \mathbf{y}^{(I_j)}_j$, where $\mathbf{y}^{(i)}_j$ spans the same temporal interval as $\mathbf{x}^{(i)}_j$. Given these group trajectories, the individual trajectory segments are mutually independent, so that

$$p(\mathbf{y}_j \mid \mathbf{X}_j, \mathbf{C}_{(j)}) = \prod_{i=1}^{I_j} p(\mathbf{y}^{(i)}_j \mid \mathbf{x}^{(i)}_j, a^{(i)}_{(j)}), \tag{5}$$

where $a^{(i)}_{(j)}$ is the label of the ith activity in sequence $\mathbf{C}_{(j)}$.

We also use a Gaussian process for individual trajectories, but fix the mean to the (given) group trajectory, i.e. $\mathbf{y}^{(i)}_j \sim \mathcal{GP}(\mathbf{x}^{(i)}_j, \kappa)$, which implies that $\mathbf{y}^{(i)}_j \sim \mathcal{N}(\mathbf{x}^{(i)}_j, \mathbf{K}^{(i)}_j)$, where the ijth entry in $\mathbf{K}^{(i)}_j$ is the covariance function κ evaluated at the ith and jth frames of $\mathbf{y}^{(i)}_j$, using the scale corresponding to the activity label associated to $\mathbf{x}^{(i)}_j$. See Figure 4 for an example graphical model of this distribution.

3.4 Specific Activities

In this work, we limit ourselves to six specific activities, three intentional (FREE-FOR-ALL, MEET, and MOVE-TO) and three physical (STAND, WALK, and RUN). FFA has a single role which allows all activities to take place. A MEET activity assigns non-zero probability to two roles, APPROACHER and WAITER; an APPROACHER performs a MEETs (recursively) and MOVE-TOs, and a WAITER only performs STANDs. MOVE-TO only produces one role, MOVER, which switches uniformly at random between the three physical activities. Finally, the physical activities have scale parameters such that $\sigma_{\text{STAND}} < \sigma_{\text{WALK}} < \sigma_{\text{RUN}}$.

4 Inference

Given a set of J individual trajectories $\mathbf{Y} = (\mathbf{y}_1, \ldots, \mathbf{y}_J)$, such as those depicted in Figure 1(c), we wish to find an activity tree Λ, such as that depicted in Figure 1(a), that best describes them. Specifically, we wish to maximize the posterior probability of an activity tree given the observed data

$$p(\Lambda \mid \mathbf{Y}) \propto p(\Lambda) p(\mathbf{Y} \mid \Lambda), \tag{6}$$

where the prior is given by (2), and the likelihood is

$$p(\mathbf{Y} \mid \Lambda) = \int p(\mathbf{X} \mid \Lambda) \prod_{j=1}^{J} p(\mathbf{y}_j \mid \mathbf{X}_j, \mathbf{C}_j) \, \mathrm{d}\mathbf{X}. \tag{7}$$

The integrands are given by (4) and (5). In general, the integral in (7) cannot be computed analytically. However, since every factor in (7) is a normal pdf, $p(\mathbf{Y} \mid \Lambda)$ is also normal, which makes the evaluation of (6) straightforward.

We cannot find $\Lambda^* = \arg\max_\Lambda p(\Lambda \mid \mathbf{Y})$ analytically. Instead, we draw S samples from the posterior (6) using the Metropolis-Hastings (MH) algorithm, and keep the sample with the highest posterior probability. At the ith iteration, we draw Λ' from a proposal distribution $q(\cdot \mid \Lambda^{(i-1)})$, where $\Lambda^{(i-1)}$ is the current sample, and accept the sample with the standard MH acceptance probability (Neal 1993).

The ability of MH to efficiently explore the space depends largely on the choice of the proposal distribution q. Although there has been work on MCMC sampling on tree models (Chipman, George, and McCulloch 2002; Pratola 2013) there is no general approach which can be applied to any model. Consequently, we employ a proposal distribution which is specific to our model.

4.1 Proposal distribution

Our proposal mechanism is composed of sampling moves which perform edits to the current hypothesized activity tree to produce a new tree sample. When drawing a sample from q, we choose a move uniformly at random to apply. When applying a move, we must make sure that the resulting tree is valid (e.g., start and end times must be consistent; or activity sequences must be possible given the role), which requires book-keeping that is beyond the scope of this document.

We have also developed a set of bottom-up activity detectors to help explore the space efficiently. These detectors provide rough estimates of groupings of individuals at each frame, and activities being performed by each group (see Section 4.1, "Detectors"). We use these detectors in two ways. First, we initialize the sampler to a state obtained by transforming the output of the detectors to an activity tree $\Lambda^{(0)}$. Additionally, we bias our proposal distribution toward groups and activities found by the detectors. For example, when proposing a *merge* move, we might choose participants which are predicted to be in a group by some activity detector.

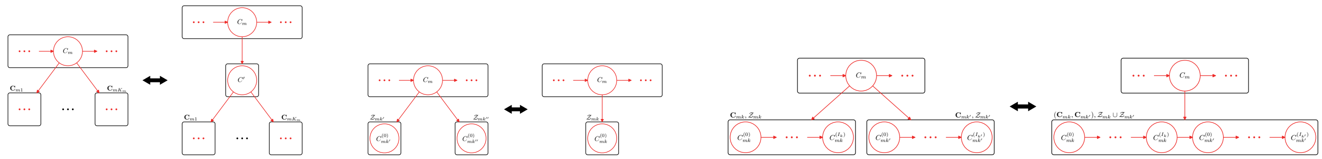

(a) Birth/death (b) Merge/split (c) Sequence/unsequence

Figure 5: An illustration of our sampling moves. (a) The birth move (left to right) inserts an intentional activity C' between sequences $\mathbf{C}_{m1}, \ldots, \mathbf{C}_{mK_m}$ and their parent C_m. In the death move, the opposite operation is performed. (b) In the merge move (left to right), children $C^{(0)}_{mk'}$ and $C^{(0)}_{mk''}$ of intentional activity C_m (and members of single-activity sequences), with $a^{(0)}_{mk'} = a^{(0)}_{mk''}$, are replaced by a single activity node $C^{(0)}_{mk}$, with activity $a^{(0)}_{mk'}$, and participant set $\mathcal{Z}_{mk'} \cup \mathcal{Z}_{mk''}$. In the reverse move, $C^{(0)}_{mk}$ is split into two nodes, both with activity label $a^{(0)}_{mk}$, with $\mathcal{Z}_m$ randomly partitioned. (c) In this example, a sequence move (left to right) takes two child sequences of intentional activity node C_m, $\mathbf{C}_{mk}$ and $\mathbf{C}_{mk'}$, and forms a single sequence $(\mathbf{C}_{mk}, \mathbf{C}_{mk'})$ with participant set $\mathcal{Z}_{mk} \cup \mathcal{Z}_{mk'}$. In the reverse move, we randomly choose a split point in the activity sequence on the right, and create two separate sequences under the same parent C_m.

Sampling moves During inference, we employ the following moves (see Figure 5 for an illustration). (a) **Birth/death**: a birth move inserts an intentional activity node between an intentional activity and some of its children. We randomly choose a set of sibling activity sequences $\mathbf{C}_{m1}, \ldots, \mathbf{C}_{mK_m}$ whose parent is intentional activity C_m, and insert a new intentional activity node C' (whose label is also chosen at random), such that C' becomes the parent of $\mathbf{C}_{m1}, \ldots, \mathbf{C}_{mK_m}$ and a child of C_m. In a death move, we randomly choose a intentional node C', remove it from the tree, and connect its children nodes to its parent. (b) **Merge/split**: In a merge move, we take two sibling activity nodes with the same label and combine them into a single activity. If C' and C'' are two activities with label a and groups $\mathcal{Z}'$ and $\mathcal{Z}''$, we create a new node C with label a and participants $\mathcal{Z}' \cup \mathcal{Z}''$. The split move performs the opposite operation, taking a-labeled node C and splitting it into two nodes C' and C'', both with activity a, assigning participants in $\mathcal{Z}$ to either $\mathcal{Z}'$ or $\mathcal{Z}''$ uniformly. (c) **Sequence/unsequence**: Let $\mathbf{C}_1$ and $\mathbf{C}_2$ be two temporally non-overlapping sibling activity sequences. A sequence move concatenates $\mathbf{C}_1$ and $\mathbf{C}_2$ into a new sequence $\mathbf{C}$. An unsequence move randomly selecting a split point at which to separate a sequence. (d) **Relabel move**: The relabel move randomly changes C's label. Note that the label must be valid, e.g., we cannot assign a physical activity label to an intentional activity node.

Detectors The bottom-up detectors provide an estimate of how individuals in the video are grouped across time, as well as the physical activity they are performing.

At each frame, we cluster individuals into groups using their trajectories on the ground plane. We apply the density-based spatial clustering of applications with noise (DBSCAN) (Ester et al. 1996) algorithm independently on each frame, where our feature is composed of the position and velocity of an individual at that frame, both of which are obtained from the smoothed trajectories (which are assumed to be given). Importantly, we keep track of individual identities over time by recording the actors involved in each group in the previous frame and assigning the cluster found in the following frame where the majority of individuals in that new set are still involved. Given the groups as computed above, we want to identify the physical activities of their individuals (e.g., WALK, RUN). For this we use a hidden Markov model, where the observation function is a naive Bayes model with each individual's speed modeled by a Gamma distribution, and a transition function that prefers staying within the current activity.

5 Experiments and Results

We evaluate the model in two ways. First, we demonstrate the model's expressive power in inferring two different types of complexly structured scenarios from synthetic data. In the first, groups of individuals engage in activities and disband, forming different groups over time. The second demonstrates a recursively structured activity, in which one meeting is a component of a higher-level meeting. We then evaluate the model on real data; specifically on two publicly available group activity datasets, VIRAT (Oh et al. 2011) and the UCLA aerial event dataset (Shu et al. 2015).

5.1 Evaluation

Performance is measured in terms of how well activities are labeled in the scene, and how well individuals are grouped, irrespective of activity label. In the following, Λ_{gt} and Λ are the ground truth and inferred activity trees, respectively.

Activity Labeling For each activity a and video frame f, we compare between Λ_{gt} and Λ the set of individuals performing a at f. We first define performance counts in terms of an individual at a frame, then compute overall counts and associated performance measures.

For an individual j at frame i, let λ_{ji} be the set of individuals which have the same label as j in Λ. Define λ'_{ji} similarly for Λ_{gt}. The set of false positives for j is $\lambda_{ji} \setminus \lambda'_{ji}$, the set of false negatives is $\lambda'_{ji} \setminus \lambda ji$, the true positives are $\lambda'_{ji} \cap \lambda_{ji}$, and the true negatives are $(\mathcal{Z} \setminus \lambda_{ji}) \cap (\mathcal{Z} \setminus \lambda'_{ji})$, where $\mathcal{Z}$ is the set of all individuals.

Grouping We follow a similar approach when evaluating grouping performance. For person j, we compare the groups to which j belongs in Λ_{gt} and Λ at each frame t. Since the

(a) VIRAT frames

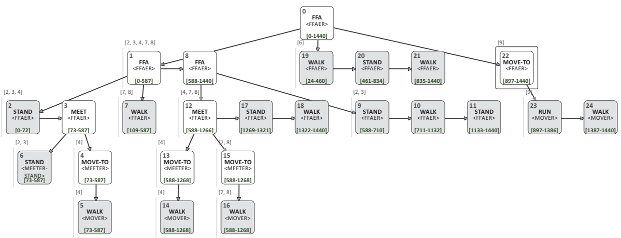

(b) Inferred activity tree

Figure 6: Qualitative results the VIRAT dataset. (a) shows two frames of the VIRAT2 video. Red boxes represent tracked individuals, gray rectangles indicate groups of individuals, and white boxes contain information such as track id, etc. In (b) we show the inferred activity tree, illustrated in a similar way as in Figure 1(a).

two trees could have different depths and topologies, it is not necessarily clear which groups should be compared with which; however, every individual is part of exactly one physical activity group at each frame, as well as one highest level node. Consequently, we only compare groups at these two levels of the tree, without penalty for difference in activities within a level. Thus once we determine the group associated with person j at frame t at the physical (resp. highest) activity level of each tree, we compute the score as before.

5.2 Results

The performance of our algorithm is summarized in Tables 1 and 2. Table 1 shows the activity labeling precision and recall on the two synthetic scenes (SYNTH1 and SYNTH2), a video sequence obtained from the VIRAT dataset, and four different video sequences from the UCLA aerial event dataset (UAED). In Table 2 we see the performance as measured by our grouping evaluation metric described above.

Synthetic data The synthetic dataset comprises two videos, where a video is a set of trajectories on the ground plane. In the first, SYNTH1, five actors participate in a series of meetings, where participants repeatedly change group memberships across 20 frames. The second (SYNTH2) features five actors meeting, with four of them participating in a side meeting before joining the global meeting. As Table 1 shows, our model performs very well on high-level activities, such as MEET, even when presented with nested structure.

VIRAT We also evaluate on real data, specifically frames 2520 to 3960 of video 2 of the VIRAT dataset. This video features seven people participating in two meetings, where groups exchange members several times. Fig. 6 shows two frames of the video, along with the inferred activity tree. Our model correctly recognizes the two meetings, as well as all of the groups at the highest level of description. The activity labeling results (Table 1) show perfect FFA performance, and the grouping results (Table 2) show a perfect highest-level intentional activity score. As before, there is divergence from ground truth at the physical activity level, but this does not affect the grouping score.

SYNTH1	STAND	WALK	MOVE-TO	MEET	FFA
Precision	0.59	0.84	0.63	0.71	1.00
Recall	1.00	0.94	0.71	0.75	1.00
F1	0.74	0.88	0.67	0.73	1.00
SYNTH2	STAND	WALK	MOVE-TO	MEET	FFA
Precision	0.87	1.00	0.94	1.00	×
Recall	0.50	0.71	0.73	0.56	×
F1	0.63	0.83	0.82	0.72	×
VIRAT	STAND	WALK	MOVE-TO	MEET	FFA
Precision	0.85	0.81	0.73	0.90	1.0
Recall	0.51	0.88	0.89	0.80	1.0
F1	0.64	0.85	0.81	0.85	1.0
UAED	STAND	WALK	MOVE-TO	MEET	FFA
Precision	0.96	0.89	0.71	0.75	0.97
Recall	0.82	0.99	0.67	0.64	0.73
F1	0.86	0.94	0.62	0.62	0.77

Table 1: Activity labeling results for synthetic videos SYNTH1 and SYNTH2, and the VIRAT and UCLA aerial event datasets. Each table shows precision, recall, and F1 for each activity. See Section 5.1 for details.

	SYNTH1		**SYNTH2**		**VIRAT**		**UAED**	
	PHYS	INT	PHYS	INT	PHYS	INT	PHYS	INT
Precision	0.86	1.0	1.00	1.0	0.98	1.0	0.95	0.93
Recall	1.00	1.0	0.69	1.0	0.85	1.0	0.99	0.89
F1	0.92	1.0	0.82	1.0	0.91	1.0	0.97	0.89

Table 2: Grouping precision, recall, and F1 scores for the synthetic videos and the two datasets VIRAT and UCLA aerial event dataset (UAED). See Section 5.1 for details.

UCLA aerial event dataset We extracted four video sequences from the UCLA aerial event dataset (UAED). More specifically, we searched for subsequences of videos which featured properties like activity nesting, groups interchanging members, etc. The result is four video sequences of roughly 2000 frames each. As we can see in Table 1, which shows the overall precision and recall scores, for all four videos, our algorithm performs reasonably well across all activities. Note the relatively low recall score of the MEET activity, which is due in large part to one very long missed MEET in the third video sequence. Similarly, Table 2 shows that our algorithm performs well at finding groups of individuals at both the physical and intentional activity levels.

6 Discussion

We have presented a probabilistic generative model of complex multi-agent activities over arbitrary time scales. The activities specify component roles between groups of actors and accommodate unboundedly deep recursive, hierarchical structure. The model accommodates arbitrary groups participating in activity roles, describing both between-group and between-individual interactions. Physical and intentional (higher-level description) activities explain hierarchical correlations among individual trajectories. To our knowledge, no existing model of track-based activity recognition provides this expressiveness in a joint model.

The modeling framework is naturally extensible. We are currently undertaking several extensions, including (1) developing additional activities, including following, exchanging items, and interacting with vehicles and building entrances, (2) adding prior knowledge about the spatial layout of the scene that naturally constrains what activities are possible, such as roads, sidewalks, impassible buildings, and other spatial features that influence behavior in order to improve both accuracy and speed by reducing the search space, (3) using our model as a prior for a 3D Bayesian tracker (Brau et al. 2013), and (4) connecting natural language to activity descriptions as our model accommodates activity descriptions across multiple events, tracking individual participation throughout, providing opportunities for building natural language narratives about activities at different levels of granularity.

Acknowledgements

This research was supported by grants under the DARPA Mind's Eye program W911NF-10-C-0081 (subcontract to iRobot, 92003) and the DARPA SSIM program W911NF-10-2-0064. We give special thanks to Paul R. Cohen and Christopher Geyer for helpful discussions and advice.

References

Aggarwal, J. K., and Ryoo, M. S. 2011. Human activity analysis: A review. *ACM Computing Surveys (CSUR)* 43(3).

Barbu, A.; Bridge, A.; Burchill, Z.; Coroian, D.; Dickinson, S.; Fidler, S.; Michaux, A.; Mussman, S.; Siddharth, N.; Salvi, D.; Schmidt, L.; Shangguan, J.; Siskind, J. M.; Waggoner, J.; Wang, S.; Wei, J.; Yin, Y.; and Zhang, Z. 2012. Video in sentences out. In *UAI 2012*.

Brau, E.; Guan, J.; Simek, K.; del Pero, L.; Dawson, C. R.; and Barnard, K. 2013. Bayesian 3d tracking from monocular video. In *ICCV 2013*.

Chang, M.-C.; Krahnstoever, N.; Lim, S.-N.; and Yu, T. 2010. Group level activity recognition in crowded environments across multiple cameras. In *AVSS*, 56–63.

Chang, M.-C.; Krahnstoever, N.; and Ge, W. 2011. Probabilistic group-level motion analysis and scenario recognition. In *ICCV 2011*, 747–754. IEEE.

Cheng, Z.; Qin, L.; Huang, Q.; Yan, S.; and Tian, Q. 2014. Recognizing human group action by layered model with multiple cues. *Neurocomputing* 136:124–135.

Chipman, H.; George, E.; and McCulloch, R. 2002. Bayesian treed models. *Machine Learning* 48(1-3):299–320.

Choi, W., and Savarese, S. 2012. A unified framework for multi-target tracking and collective activity recognition. In *ECCV 2012*, 215–230.

Ester, M.; peter Kriegel, H.; S, J.; and Xu, X. 1996. A density-based algorithm for discovering clusters in large spatial databases with noise. 226–231. AAAI Press.

Garate, C.; Zaidenberg, S.; Badie, J.; and Bremond, F. 2014. Group tracking and behavior recognition in long video surveillance sequences. In *VISIGRAPP 2014*.

Geib, C. W., and Goldman, R. P. 2009. A probabilistic plan recognition algorithm based on plan tree grammars. *Artificial Intelligence* 173:1101–1132.

Kwak, S.; Han, B.; and Han, J. H. 2013. Multi-agent event detection: localization and role assignment. In *CVPR*.

Lan, T.; Wang, Y.; Yang, W.; and Mori, G. 2010. Beyond actions: Discriminative models for contextual group activities. In *Advances in neural information processing systems*, 1216–1224.

Lan, T.; Sigal, L.; and Mori, G. 2012. Social roles in hierarchical models for human activity recognition. In *CVPR*.

Lin, W.; Sun, M.-T.; Poovendran, R.; and Zhang, Z. 2010. Group event detection with a varying number of group members for video surveillance. *Circuits and Systems for Video Technology, IEEE Transactions on* 20(8):1057–1067.

Neal, R. M. 1993. Probabilistic inference using markov chain monte carlo methods. Technical report.

Odashima, S.; Shimosaka, M.; Kaneko, T.; Fukui, R.; and Sato, T. 2012. Collective activity localization with contextual spatial pyramid. In *Computer Vision–ECCV 2012. Workshops and Demonstrations*, 243–252. Springer.

Oh, S.; Hoogs, A.; Perera, A.; Cuntoor, N.; Chen, C.-C.; Lee, J. T.; Mukherjee, S.; Aggarwal, J.; Lee, H.; Davis, L.; et al. 2011. A large-scale benchmark dataset for event recognition in surveillance video. In *CVPR 2011*, 3153–3160. IEEE.

Poppe, R. 2010. A survey on vision-based human action recongition. *Journal of Image and Vision Computing* 28(6):976–90.

Pratola, M. T. 2013. Efficient metropolis-hastings proposal mechanisms for bayesian regression tree models.

Rasmussen, C. E., and Williams, C. K. I. 2006. *Gaussian Processes for Machine Learning*. The MIT Press.

Ryoo, M. S., and Aggarwal, J. K. 2011. Stochastic representation and recognition of high-level group activities. *International Journal of Computer Vision* 93(2):183–200.

Shu, T.; Xie, D.; Rothrock, B.; Todorovic, S.; and Zhu, S.-C. 2015. Joint inference of groups, events and human roles in aerial videos. In *CVPR*.

Sukthankar, G.; Goldman, R. P.; Geib, C. W.; Pynadath, D. V.; and Bui, H. H., eds. 2014. *Plan, Activity, and Intent Recognition: Theory and Practice*. Morgan Kaufmann.

Vishwakarma, S., and Agrawal, A. 2013. A survey on activity recognition and behavior understanding in video surveillance. *The Visual Computer* 29(10):983–1009.

Zaidenberg, S.; Boulay, B.; and Bremond, F. 2012. A generic framework for video understanding applied to group behavior recognition. In *AVSS*, 136–142. IEEE.

Zhang, C.; Yang, X.; Zhu, J.; and Lin, W. 2012. Parsing collective behaviors by hierarchical model with varying structure. In *ACMMM 2012*, 1085–1088. ACM.

Zhang, Y.; Qin, L.; Yao, H.; Xu, P.; and Huang, Q. 2013. Beyond particle flow: Bag of trajectory graphs for dense crowd event recognition. In *ICIP*, 3572–3576.

Zhu, G.; Yan, S.; Han, T. X.; and Xu, C. 2011. Generative group activity analysis with quaternion descriptor. In *Advances in Multimedia Modeling*. Springer. 1–11.